Elastic Scattering of 40-Mev Alpha Particles from Heavy Elements*

H. E. WEGNER, R. M. EISBERG, AND G. IGO
Brookhaven National Laboratory, Upton, Long Island, New York
(Received April 8, 1955)

Angular distributions have been measured for the elastic scattering of 40-Mev alpha particles from Ta, Au, Pb, and Th in the angular range 21° to 155°. If the ratios of the measured cross sections to the Coulomb cross section are assumed equal to 1.0 at small angles, they increase slightly with increasing angle, and in the vicinity of 30° decrease exponentially with increasing angle to values less than 0.001. These data are compared with the semiclassical, strong absorption model of Blair and with the recent model of Ford and Wheeler.

1. INTRODUCTION

THE elastic scattering of alpha particles is one of the oldest subjects of investigation in nuclear physics. Rutherford and others,[1] using alpha particles from naturally radioactive sources, demonstrated that the scattering from nuclei could be explained by a theoretical description employing classical trajectories in a Coulomb field. However, the theory could not account for the scattering from H and He, or for the scattering at large angles from Mg and Al. It is of interest to investigate the deviations from Coulomb scattering, since such a study could be expected to yield information about the size of the nucleus, the size of the alpha particle, and about the interaction of the alpha particle with the nucleus. These experiments require more energetic alpha particles than are available from radioactive sources.

Recently, several experiments have been performed using high-energy alpha-particle beams from cyclotrons. These experiments include: the energy dependence, from 13 to 42 Mev, of the cross section for the elastic scattering of alpha particles,[2] angular distributions for elastic scattering of 22-Mev alpha particles from heavy elements,[3] and the angular distribution for elastic scattering of 28-Mev alpha particles from Au.[4]

When measured as a function of energy, the cross section is observed to agree with the energy dependence predicted by the Coulomb formula for energies below a certain critical energy, E_c. For energies greater than E_c, the cross section decreases exponentially to values less than 0.1 of the Coulomb cross section. In the heaviest elements, the cross section increases slightly above the Coulomb cross section before suddenly decreasing. The angular distributions also show an exponential decrease in cross section at angles greater than a certain critical angle, and in the heavier elements, a similar increase before the decrease.

Blair has interpreted the energy dependence of the elastic scattering cross section by using a semiclassical, strong absorption model.[5] The outgoing lth partial wave is assumed to vanish if the apsidal distance of the corresponding classical trajectory is less than the sum of the radius of the nucleus plus the radius of the alpha particle. Partial waves, corresponding to classical trajectories with larger apsidal distances, have phases characteristic of Coulomb scattering. This model can be made to fit the small increase in the cross section and part of the subsequent exponential decrease by assuming the radius of the alpha particle to be 2×10^{-13} cm and the radius of the nucleus to be $1.5\times10^{-13}A^{\frac{1}{3}}$ cm.

The angular distribution data has been interpreted by Wall, Rees, and Ford by using a modification of Blair's semiclassical strong absorption model.[3] These authors have smoothed out the abrupt spatial transition between complete absorption and no absorption by allowing the outgoing partial wave, corresponding to a grazing classical trajectory, to have the Coulomb phase and an amplitude of 0.5 times the Coulomb amplitude. This modification reduces the diffraction oscillations in the differential cross section which are not found experimentally.

Another interpretation of the energy dependence of the cross section has been advanced by Izumo.[6] He has calculated the elastic scattering cross section using the Montroll-Greenberg variational method[7] and a potential that consists of a complex square well plus a Coulomb potential. The calculation can be made to fit the experimental results if the imaginary part of the square well has a strong dependence on both the energy of the alpha particle and the scattering angle.

The region of poorest agreement between the Blair model and experiment is the region where the measured cross section is small compared to the Coulomb cross section. (In this region the model would not be expected to give quantitative agreements.) In the energy-dependence experiments, at cross sections less than about 0.1 of the Coulomb cross section, the

* Research performed under the auspices of the U. S. Atomic Energy Commission.

[1] An excellent survey of the early work of Rutherford and others with a complete index of references is contained in the book by Rutherford, Chadwick, and Ellis, *Radiations from Radioactive Substances* (MacMillan Company, Cambridge, 1930).

[2] G. W. Farwell and H. E. Wegner, Phys. Rev. **93**, 356 (1954); **95**, 1212 (1954).

[3] Wall, Rees, and Ford, Phys. Rev. **97**, 726 (1955).

[4] H. E. Gove, Massachusetts Institute of Technology (LNSE) Progress Report, May, 1951 (unpublished).

[5] J. S. Blair, Phys. Rev. **95**, 1218 (1954).

[6] K. Izumo, Progr. Theoret. Phys. (Japan) **12**, 549 (1954).

[7] E. W. Montroll and J. M. Greenberg, Phys. Rev. **86**, 889 (1952).

strong absorption model predicts that the cross section should begin to decrease less rapidly than the observed exponential decrease. However, the experimental cross section continues to decrease in this region until, at the highest energies measured, it has a value several times smaller than the theoretical prediction. A similar situation exists in the case of the angular distributions. The experimental cross section decreases exponentially with increasing angle to values less than 0.1 times the Coulomb cross section. In the case of Ag, the lightest element investigated, the experimental cross section decreases to approximately 0.01 times the Coulomb cross section. In contrast, the cross section, predicted by either the Blair model or the modified Blair model, decreases to values of the order of 0.1 times the Coulomb cross section and then oscillates violently, finally increasing towards the Coulomb cross section at 180°.

The purpose of this experiment is to extend the measurements on the angular distribution for elastic scattering from heavy nuclei to higher alpha-particle energies in order to determine whether or not the cross section continues to decrease rapidly.

The results of the experiment show that the cross section does continue to decrease rapidly to values less than three orders of magnitude smaller than the Coulomb cross section. There is no evidence for an increase in the cross section at very large angles. These data are compared with the predictions of the Blair models and are shown to be in striking disagreement in the region where the measured cross section is small compared to the Coulomb cross section. In view of the approximations in the theory this disagreement is not surprising.

After the experiment was completed, the authors were informed of some unpublished calculations by Ford and Wheeler on the elastic scattering of alpha particles.[8] These calculations are based on a model in which the surface of the nucleus is transparent to the alpha particle. The assumptions which enter into the theory are best satisfied for large alpha-particle energy and large scattering angles. At these angles the theory predicts that the cross section drops monotonically to very small values, which is in qualitative agreement with the results of this experiment.

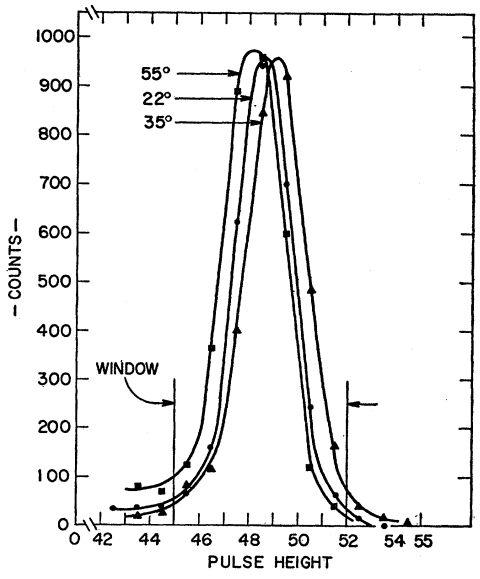

FIG. 1. Pulse-height distributions at 22°, 35°, and 55°.

2. EXPERIMENTAL PROCEDURE

For these experiments, the external alpha-particle beam of the Brookhaven 60-inch cyclotron is directed into an evacuated beam pipe. The beam pipe follows the trajectory of the alpha particles through the fringing field of the cyclotron magnet and then passes through a two-element magnetic strong-focusing lens of 2-inch aperture,[9] located 4 feet from the cyclotron vacuum chamber. The beam pipe then passes through a channel in a shielding wall and terminates at a scattering chamber located 30 feet from the cyclotron. The alpha-particle beam travels through the evacuated pipe and is brought to a focus on a thin target at the center of the scattering chamber. The focused beam forms an approximately circular spot $\frac{1}{4}$ inch in diameter. The current in the beam is 10% to 20% of the total deflected cyclotron beam and 1% to 2% of the circulating beam. Focused alpha-particle beams in excess of 5 microamperes have been obtained. In this experiment, the beam is further defined by a $\frac{1}{8}$-inch tantalum diaphragm located 10 inches in front of the target.

Particles which are scattered from the target foil into the horizontal plane of the one-foot diameter evacuated scattering chamber pass through exit windows of low areal density and are detected. The windows are arranged so that measurements can be made at any angle from 20° to 160°. A movable frame holding three targets is supported at the center of the chamber. The chamber is positioned so that the alpha-particle beam is accurately aligned with respect to the axis of the chamber and with respect to a graduated circle engraved on the outside of the chamber, used to measure the scattering angle.

After traversing the scattering chamber, the beam is stopped in a Faraday cup. The Faraday cup current is used by the operator to tune the cyclotron. The beam monitor used in the experiment is a NaI scintillation counter which detects alpha particles elastically scattered from the target at a fixed angle of 26°. This monitor provided a linear and reproducible measure of the integrated beam.

The energy of the beam is determined by measuring the range in aluminum of alpha particles elastically scattered from a target of high atomic weight. The energy is 41±0.3 Mev.

[8] K. W. Ford and J. A. Wheeler (to be published).
[9] B. Cork and E. Zajec, University of California Radiation Laboratory Report No. 2182 (unpublished).

A second NaI scintillation counter, mounted on an arm which rotates about the center of the scattering chamber, is used to measure the angular distribution of the alpha particles elastically scattered from the target foil. Pulses from the detector pass through a cathode follower and into a linear amplifier. The output of the linear amplifier passes into a pulse-height analyzer.

The pulse-height distribution from the detector consists of a continuum and a sharp peak. The sharp peak contains the elastically scattered alpha particles. The continuum contains inelastically scattered alpha particles and other particles, such as protons, which result from alpha-induced reactions. The continuum extends to pulse heights greater than the pulse height of the elastic alpha-particle peak because protons lose less energy traversing the target and the scattering chamber window, and because of the nonlinear responses of NaI for alpha particles. The ratio of the area under the elastic alpha particle peak to the area under the continuum depends upon the scattering angle. At forward angles, the continuum is negligible; as the scattering angle increases, the elastic alpha-particle peak decreases relative to the continuum, until it vanishes into the continuum at large angles.

Due to the rapid change of the character of pulse-height distribution with increasing scattering angle, two methods were used to separate the elastically scattered alpha particles from the continuum. For scattering angles less than 55°, where the continuum is very small, an Atomic Instrument Company single-channel pulse-height analyzer was adjusted so that the acceptance window encompassed the elastic alpha-particle peak. Figure 1 shows pulse-height distributions for particles scattered from a thin Au target at three forward angles. The slight shift in the location of the peak with scattering angle is due to the change, with angle, in the amount of material which the alpha particles must penetrate in traversing the scattering chamber window. The vertical lines drawn at 45 and 52 volts show the acceptance window of the single-channel pulse-height analyzer.

Figure 2 shows pulse-height distributions for alpha particles scattered from a thin Ta target at three large angles. These curves show that at these angles it is necessary to measure the differential pulse-height distribution at each scattering angle in order to correctly subtract the continuum from the elastic alpha-particle peak. Data were obtained at scattering angles greater than 55° with an Atomic Instrument Company 20-channel pulse-height analyzer. The elastic scattering cross section was assumed to be proportional to the area between the elastic peak and the continuum. The straight lines shown in Fig. 2 indicate this subtraction.

The elastic scattering cross section decreases rapidly with increasing scattering angle; the cross section drops by approximately six orders of magnitude over the range measured. In order to maintain a reasonable

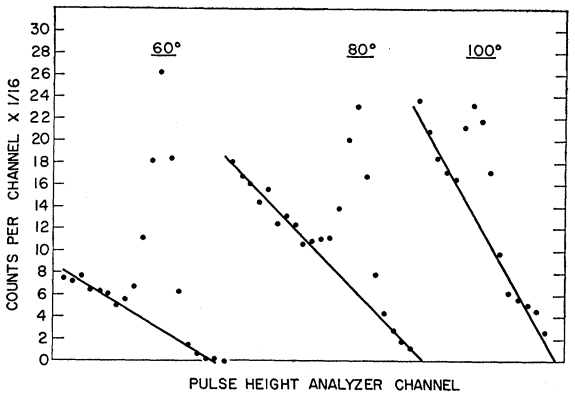

FIG. 2. Pulse-height distributions at 60°, 80°, and 100°.

counting rate in the detector as the scattering angle is changed, it is necessary to vary the intensity of the incident alpha-particle beam and the solid angle subtended by the detector. A variation of nearly two orders of magnitude can be made in the beam intensity by adjusting the strong focusing lens. The solid angle subtended by the detector is varied over a range of two orders of magnitude by changing the size of a diaphragm placed in front of the detector.

The data for each element investigated were obtained in five groups, each group spanning a restricted range of angle. The experimental conditions differed from one range to another, i.e., the single-channel pulse-height analyzer was used in some ranges while the 20-channel pulse-height analyzer was used in others, and also the diaphragm in front of the detector was changed from range to range. The angular ranges were overlapped at their extremes, and the cross sections measured in a particular range were normalized at the overlapping points to the data obtained in the adjacent ranges.

3. EXPERIMENTAL RESULTS

Figure 3 shows the measured differential cross section for the elastic scattering of 40-Mev alpha particles from Ta, Au, Pb, and Th. The abscissa is the laboratory scattering angle. The ordinate is the relative differential cross section. The heavy curve represents the angular dependence of the Coulomb scattering differential cross section. Figure 4 shows an expanded view of the data of Fig. 3 in the region 21° to 40°. Typical statistical errors are shown on the Ta data. At angles less than 40° the statistical errors are smaller than the size of the points.

At sufficiently small scattering angles, the elastic scattering cross section should be equal to the Coulomb scattering cross section. It is observed that, for the first few points, the slope of the measured cross-section curves coincides with the slope of the Coulomb scattering cross-section curve. Consequently, the measured differential cross sections were assumed equal to the Coulomb differential cross section at the 21° and the

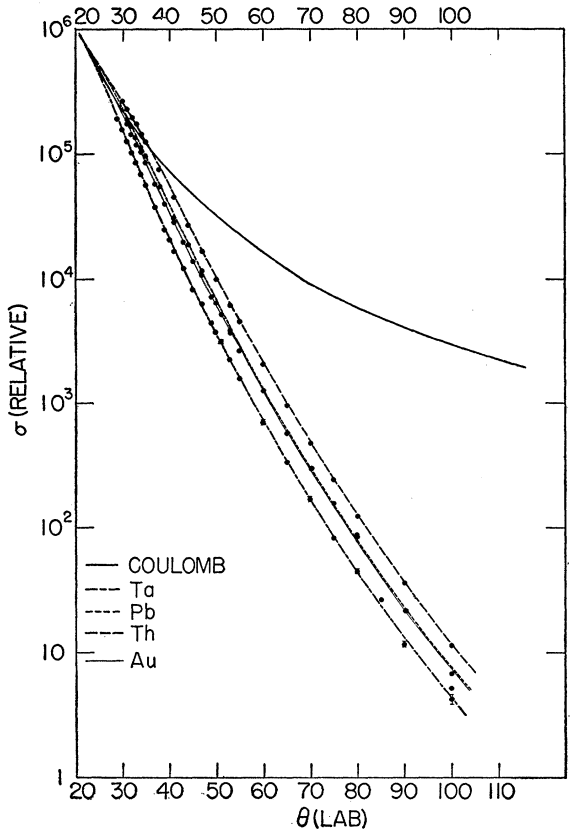

FIG. 3. Angular dependence of the elastic scattering cross section for alpha particles scattered from Ta, Pb, Th, and Au.

22° points, and the data presented in Figs. 3 and 4 have been normalized accordingly. The earlier experiments on the elastic scattering of alpha particles from heavy elements[2,3] have shown that the cross sections have an angular dependence which justifies this normalization procedure. The geometry of the scattering chamber limited the measurements to a minimum angle of 21°.

As the scattering angle increased, the measured cross sections departed from the Coulomb cross section. In the heavier elements, Au, Pb, and Th, the cross section first increased above the Coulomb cross section and then decreased rapidly. The magnitude of the increase was greater for greater atomic weights. In the case of Ta, the cross section does not initially increase as observed in the heavier elements. However, there could be an increase at angles smaller than those investigated. The observed increase, before the decrease in the cross section for the heavier elements, is in qualitative agreement with earlier experiments.

Figure 5 shows the ratio of the measured elastic scattering cross section to the Coulomb scattering cross section, σ/σ_c, plotted as a function of laboratory scattering angle. These ratios have been normalized to unity at the 21° and 22° points as discussed above. It should be noted that any errors arising from the normalization procedure will shift the curves vertically on the semilogarithmic plot but will not change their shape. Typical statistical errors are shown on the Ta data. In order to show clearly the angular dependence of σ/σ_c from 21° to 40°, the experimental points are not shown. In this region the statistical errors are less than the size of the points shown at greater angles.

In order to carry the cross-section measurements to angles larger than 100°, it is necessary to use a very thin scattering target. Such targets were available for Au. Measurements were made at 90°, 105°, 130°, and 155°. At 130° and 155°, the elastic alpha-particle peak was not distinguishable from the continuum and it was only possible to set an upper limit on the cross section. The cross section for Au continues to decrease with increasing angle; the ratio, σ/σ_c, is less than 0.0003 at 130° and 155°.

4. EXPERIMENTAL ERRORS

The alpha-particle beam passed through the axis of the scattering chamber to within 0.030 in. and was aligned with respect to the graduated circle to within 0.2°. The alignment was checked by determining the alpha-particle elastic scattering cross section at some measured angle on the left side of the chamber and then at the same measured angle on the right side of the chamber. The cross sections observed in these two cases were equal within counting statistics. This indicated that the error involved in measuring the scattering angles was less than 0.25°.

The size of the diaphragm placed in front of the detector varied from 0.040 to 0.375 in. in diameter. The width of the beam at the target foil was 0.125 in. At forward angles, where the smallest diaphragm was used, the angular resolution of the detector was limited by the width of the beam and was ±0.5°. At backward angles, where the largest diaphragm was used, the

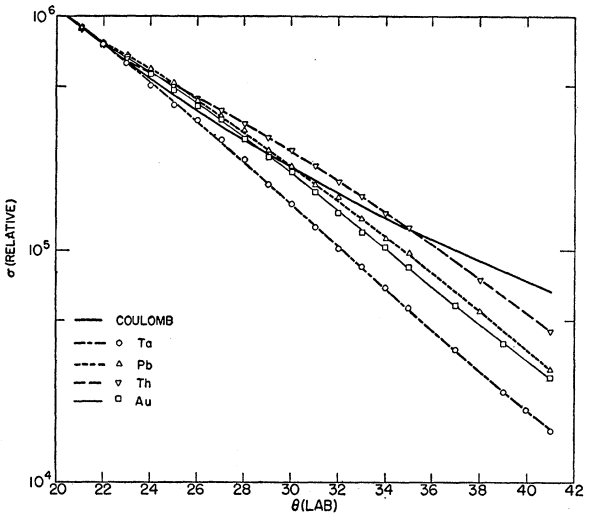

FIG. 4. Expanded view of small angle data of Fig. 3.

angular resolution was limited by the diaphragm and was $\pm 1.5°$. Since the counting rate increased rapidly with decreasing angle, a detector of finite angular resolution would measure the cross section at a somewhat smaller angle than the angle measured to the center of the diaphragm. However, a calculation showed the effect to be negligible in this experiment.

The incident alpha-particle beam lost approximately two Mev in passing through the target foils. The spread which this introduced in the energy of the alpha particles when scattering could erase very small diffraction effects. However, earlier experiments which utilized thinner targets showed no evidence of diffraction effects.[2,3] The initial energy of the beam was 41 ± 0.3 Mev, but the scattering energy should be quoted as 40 ± 1 Mev.

The counting rate of the detector, in the region of the elastic alpha-particle peak, was zero with the scattering target removed.

The error involved in monitoring the beam was determined by the counting statistics of the monitor detector, which were always less than 1%.

The data from 21° to 55° were obtained with a single-channel pulse-height analyzer. This procedure contributed error to the cross-section measurement because the continuum was not subtracted from the elastic alpha-particle peak. For the three heaviest elements, in the pulse-height region covered by the window of the pulse-height analyzer, the ratio of the counting rate due to the continuum to the counting rate due to the elastic alpha-particle peak varied from 3% at 21° to 6% at 55°. (See Fig. 1.) For Ta, the ratio was 6% at 21° and 12% at 55°. The effect of neglecting the angular variation in the relative contribution of the continuum was to gradually increase the measured cross section with increasing scattering angle. For the three heaviest elements, the cross section measured at 55° was approximately 3% too large, relative to the cross section measured at 21°. In the case of Ta, this effect increased the cross section at 55° approximately 6%, relative to the cross section at 21°. No correction was made for this effect since it was very small compared to the three orders of magnitude change in the cross section over this angular range.

At angles larger than 55°, a twenty-channel pulse-height analysis was made at each angle of observation. The contribution of the continuum was subtracted from the elastic alpha-particle peak by drawing a straight line through the points in the continuum on each side of the peak. The elastic scattering cross section was then assumed to be proportional to the area between the peak and the straight line. (See Fig. 2.) By placing a thin Al absorber between the target foil and the detector, it was possible to stop the scattered alpha particles while only slightly reducing the energy of the lighter particles which comprised the continuum. In this fashion, the shape of the continuum under the elastic alpha-particle peak was examined. It was shown

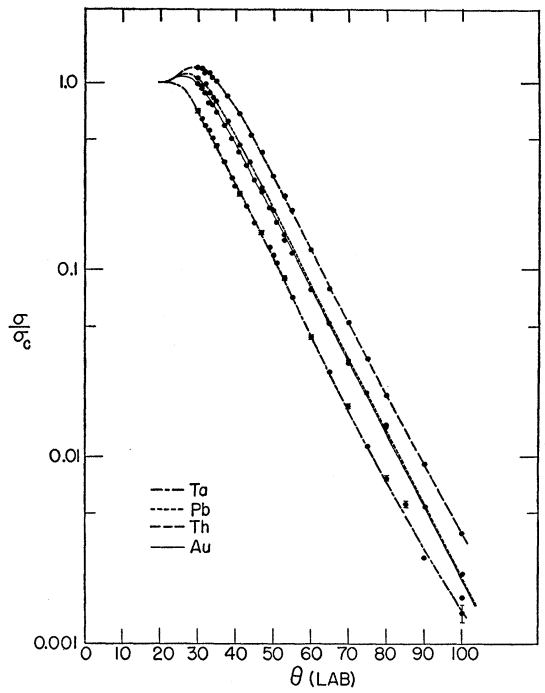

FIG. 5. Angular dependence of the ratio of the elastic scattering cross section to the Coulomb cross section, σ/σ_c, for Ta, Au, Pb, and Th.

that the continuum approximately followed the straight line interpolation. Therefore, this interpolation contributed little error.

Another possible source of error could be the presence of groups of inelastically scattered alpha particles which, within the 5% energy resolution of the detector, could not be separated from the elastically scattered alpha-particle peak. Again, comparing the continuum distribution with and without the thin Al absorber, it was possible to show, that in the region near the peak, the continuum contained few inelastically scattered alpha particles. From this it was assumed that there was a negligible number of inelastically scattered alpha particles which were not resolved from the elastic alpha-particle peak.

The statistical errors indicated for the experimental points at angles greater than 55° were determined by compounding the statistical error of the total counting rate in the peak with the statistical error involved in fitting a straight line to the continuum.

The error in normalizing the data obtained in one range of angle to the data obtained in the adjacent ranges was small compared to the statistical error of the individual points. This was a result of measuring with increased accuracy the cross section at overlapping points.

5. DISCUSSION

Under the assumptions of the Blair model[5] described in Sec. 1, the amplitude of the outgoing wave is $e^{2i\sigma l}$

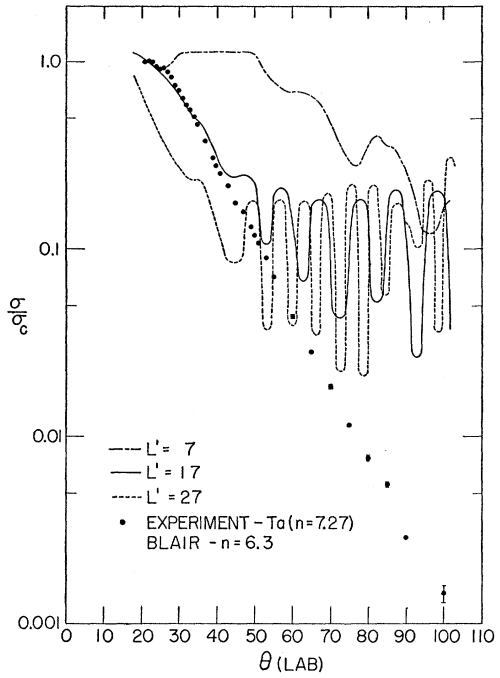

FIG. 6. Comparison of the Blair model with σ/σ_c for Ta.

for $l>l'$ and is zero for $l\leq l'$, where σ_l is the Coulomb phase. l' satisfies the equation

$$l'(l'+1)=2mR^2\hbar^{-2}(E-E_c),$$

with

$$E_c=Zze^2R^{-1}.$$

R is set equal to the radius of the nucleus plus the radius of the alpha particle; E_c is the Coulomb potential energy of a particle of charge ze at a distance R from a nucleus of charge Ze; l' is the orbital angular momentum of a particle of mass m and initial energy E.

Under the above assumptions,

$$\frac{d\sigma}{d\Omega}=\left|\frac{e^{2i\sigma_0}}{2ik}\left\{\frac{-in}{\sin^2(\theta/2)}\exp[-in\ln\sin^2(\theta/2)]-\sum_{l=0}^{l'}(2l+1)e^{2i(\sigma_l-\sigma_0)}P_l(\cos\theta)\right\}\right|^2. \quad (1)$$

The Coulomb phases are given by

$$e^{2i\sigma_l}=\Gamma(l+1+in)/\Gamma(l+1-in),$$

and

$$n=Zze^2/\hbar v.$$

The first term in Eq. (1) is the scattering due to the Coulomb potential, and the second term is due to the interaction between the nucleus and the alpha particles with $l\leq l'$. At small angles, $(\sin\frac{1}{2}\theta)^{-4}$ is large and the scattering is predominately Coulomb scattering unless l' is very large.

The modified Blair model[3] is developed in a similar manner, except that the amplitude of the outgoing wave is $0.5e^{2i\sigma l}$ for $l=l'$.

For the calculation of σ/σ_c, n is determined by the experimental conditions and l' is adjusted to fit the experimental data. The values of σ/σ_c, as a function of the scattering angle, have been tabulated for $n=6.3$, 10.6, and 11.0; and for $l'=0$ to 35 assuming the Blair model. They have also been tabulated for $n=6.3$, and 10.6; and for $l'=0$ to 23 assuming the modified Blair model. The lightest and heaviest elements investigated in this work were Ta and Th. Their respective values of n are 7.27 and 8.95. It has been shown that the theoretical predictions for the angular distribution are not strongly dependent on n.[3] Since the values of n used in the above tabulations bracket the extreme values of n in this experiment, the theoretical predictions for the angular dependence of σ/σ_c may be employed to show whether the models are capable of qualitative agreement with the experimental data.

In Fig. 6, the experimental σ/σ_c for Ta is compared with the predictions of the Blair model for $n=6.3$ and for $l'=7$, 17, and 27. In Fig. 7 the experimental σ/σ_c for Th is compared with the predictions of the Blair model for $n=10.6$ and for $l'=12$, 22, and 32. In Fig. 8 the experimental σ/σ_c for Ta is compared with predictions of the modified Blair model for $n=6.3$ and for $l'=13$ and 23. The parameter l' which fits the data best is selected by trial and error from the tabulated values, and the effect of increasing and decreasing l' is demonstrated. Because of the limited range of l' values tabulated for the modified model, it was not

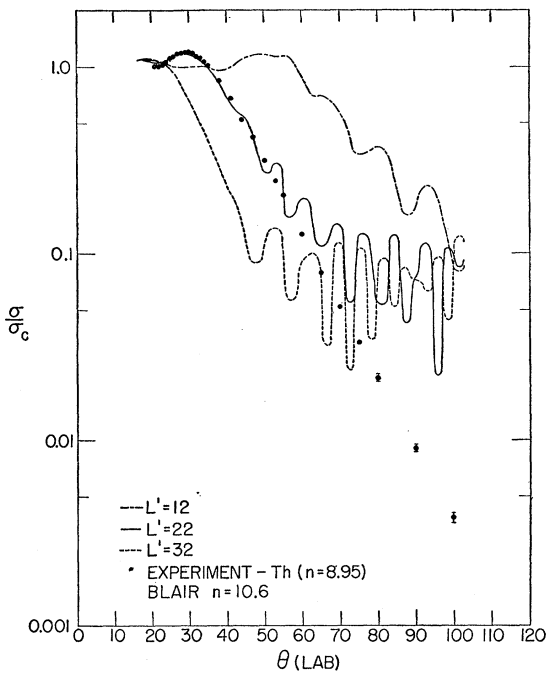

FIG. 7. Comparison of the Blair model with σ/σ_c for Th.

possible to fit the theory to the Th data or to show the effect of increasing l' to values greater than 23 for the Ta data. The l' value corresponding to the best fit for the Ta data, assuming the modified Blair model, is considerably larger than that corresponding to the best fit with the Blair model. This effect was also noted in the work of Wall, Rees, and Ford.[3]

Qualitatively, the Blair models agree with the experimental behavior of σ/σ_c for values greater than approximately 0.1. However, the experimental curve continues to decrease exponentially with increasing angle to values of σ/σ_c of the order 0.001. The theoretical curves show marked oscillations and, on the average, a gradual increase in value of σ/σ_c contrary to experiment. For Au, at angles of 130° and 155° σ/σ_c was shown to be less than 0.0003. This limit indicates that σ/σ_c does not increase in the backward direction as might be expected according to the Blair models.

The model of Ford and Wheeler[8] supposes that the potential changes gradually at the nuclear surface from strongly repulsive to strongly attractive over a number of partial waves large compared to one, and through this region the JWKB-approximate phase shift,[10] η_l, may be used:

$$\eta_l=\tfrac{1}{2}\int\theta(l)dl+\text{const.},$$

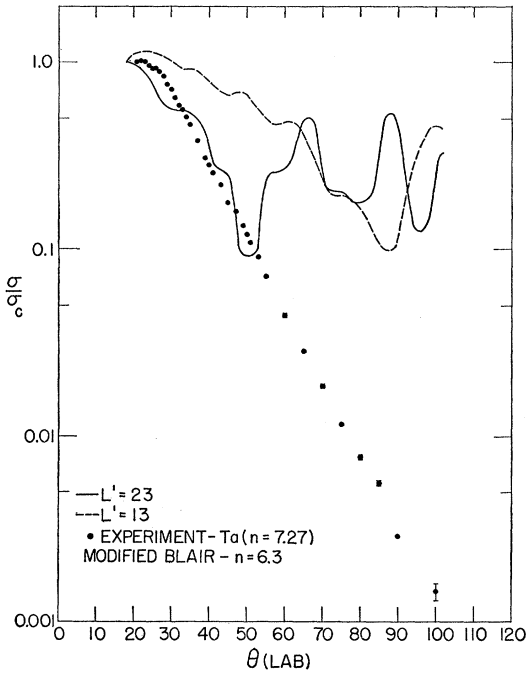

FIG. 8. Comparison of the modified Blair model with σ/σ_c for Ta.

[10] N. F. Mott and H. S. W. Massey, *The Theory of Atomic Collisions*, second edition (Clarendon Press, Oxford, 1949), p. 122.

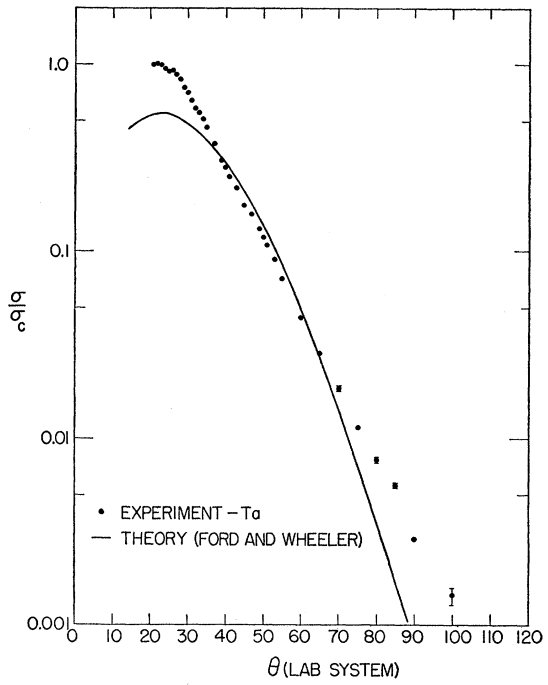

FIG. 9. Comparison of the Ford-Wheeler model with σ/σ_c for Ta.

where $\theta(l)$ is the classical deflection angle for a trajectory with angular momentum $l\hbar$. Furthermore, they suppose that the absorption may be ignored in this transition region. The form of the potential near the nuclear surface will cause the classical deflection to have a maximum, θ_1, at some critical angular momentum, l_1, near which θ will vary parabolically with l,

$$\theta\cong\theta_1-q(l-l_1)^2.$$

The JWKB cross section may then be evaluated for angles in the neighborhood of θ in terms of the adjustable parameters θ_1 and q. There is also a weak dependence on l_1, but l_1 and θ_1 will be approximately related by the Coulomb formula,

$$l_1=n\cot(\theta_1/2).$$

The result is

$$\sigma\cong\lambda\!\!\!^{-2}[2\pi(l+\tfrac{1}{2})/\sin\theta_1]q^{-\frac{2}{3}}\,\mathrm{Ai}^2\left(\frac{\theta-\theta_1}{q^{\frac{1}{3}}}\right),$$

where $\mathrm{Ai}(x)$ is the Airy integral.[11] The Coulomb cross section is evaluated at θ_1 and the relative cross section becomes

$$\sigma/\sigma_c=[2\sin^2(\tfrac{1}{2}\theta_1)/nq^{\frac{2}{3}}]2\pi\,\mathrm{Ai}^2\left(\frac{\theta-\theta_1}{q^{\frac{1}{3}}}\right).$$

This simple formula was used to fit the observed cross sections at 40 Mev for Ta($Z=73$, $n=7.27$) and for Th($Z=90$, $n=8.95$). The Ta fit is shown in Fig. 9 and

[11] H. Jeffries and B. S. Jeffries, *Methods of Mathematical Physics* (Cambridge University Press, Cambridge, 1946).

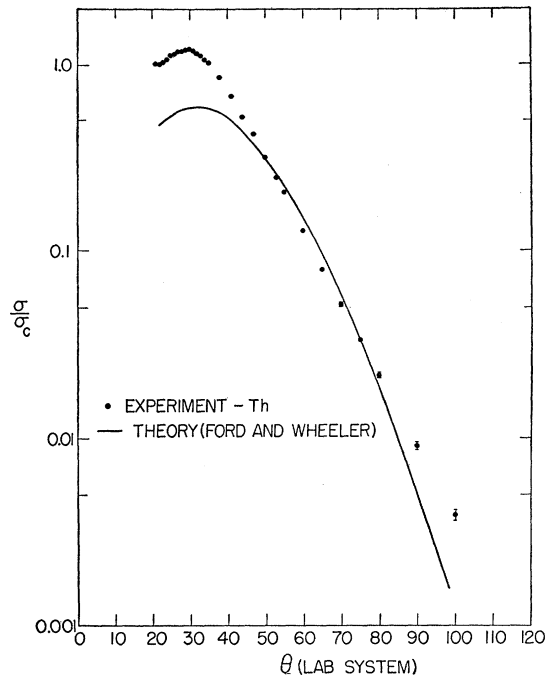

FIG. 10. Comparison of the Ford-Wheeler model with σ/σ_c for Th.

the Th fit is shown in Fig. 10. The fit is only qualitative but has the required features of a smooth and rapid decrease at angles greater than θ_1. Moreover, the determined parameters, θ_1 and q, are physically reasonable.

For Ta, the angle $\theta_1=43°$ and $l_1=18.5$. The "interaction radius", R_{int}, is defined as the point of closest approach at this angular momentum; $R_{\text{int}}=1.74\times10^{-13}A^{\frac{1}{3}}$ cm. If 2.5×10^{-13} cm is arbitrarily subtracted for the alpha particle radius, the radial constant is reduced from 1.74 to 1.30. As a measure of the surface thickness, Δl, one may define

$$\Delta l=[\theta_1/q].$$

For Ta, $q=0.0425$ radian, $\Delta l=4.2$. For Th, the fit is obtained with $\theta_1=53°$, $l_1=17.9$, and $R_{\text{int}}=1.71\times10^{-13}A^{\frac{1}{3}}$ cm. In this case, the subtraction of 2.5×10^{-13} cm from R_{int} reduces the radial constant from 1.71 to 1.30. The "surface thickness" parameter, q, is 0.0494 for Th and $\Delta l=4.3$ or about 1.3×10^{-13} cm.

The physical idea of this model is that the scattering in the region of rapid decrease of the cross section is governed by the nuclear surface region, and that this region may be "thick" ($\Delta l\gg1$) and almost nonabsorbing. The mathematical approximations are: the JWKB phase shift may be used; the classical deflection angle as a function of l is parabolic in the region of interest; the scattering amplitude sum may be replaced by an integral; the Legendre polynomials may be replaced by their asymptotic forms; and the integral may be evaluated approximately because of the condition $l_1\gg\Delta l\gg1$. These approximations lead to a very simple result. However, for the energies and angles in this experiment, it is not expected to have quantitative validity.

Previous experiments on the elastic scattering of alpha particles discussed in Sec. 1 may be compared with each other and with the results of this experiment by plotting σ/σ_c as a function of a parameter common to the various experiments. The change in linear momentum of the alpha particle upon scattering and the apsidal distance corresponding to a classical trajectory of the alpha particle are two such parameters. The change in linear momentum, Δp, is a reasonable parameter to consider because of its importance in the Born approximation. However, the results of the various experiments when plotted as a function of Δp show that σ/σ_c is not a function of Δp alone.

The results of the various experiments were plotted as a function of apsidal distance, that is, the point of nearest approach of the classical trajectory corresponding to a given energy and scattering angle. This comparison is shown in Fig. 11. The points were obtained from the following experiments on the elastic scattering of alpha particles from Au: the energy dependence in the range 13–42 Mev of the cross section for scattering at 60° and at 95°,[2] the angular dependence in the range 20–60° of the cross section for scattering at 22 Mev,[3] and the angular dependence in the range 21–100° of the cross section for scattering at 40 Mev. Plots of the various data for elastic alpha particle scattering from Th, Pb, and Ta also show agreement similar to that shown for Au. The radius of the Au nucleus, assuming $R_{\text{Au}}=1.5\times10^{-13}A^{\frac{1}{3}}$ cm, and the radius of the Au nucleus plus the radius of the alpha particle, assuming $R_\alpha=1.2\times10^{-13}$ cm, are indicated. At apsidal distances large compared to the radius of the nucleus, all the curves coincide because σ/σ_c must approach 1.0. The behavior of the curves at small apsidal distances is paradoxical because the apsidal distance is calculated by assuming the formulas for Coulomb scattering. Yet, the curves continue to coincide approximately where the Coulomb scattering formulas are not valid since $\sigma/\sigma_c<1.0$. It is clearly an important fact that the cross section qualitatively depends on the apsidal distance, but this behavior is not completely understood in terms of the present models.

In conclusion, it is of interest to see what information the elastic scattering of alpha particles has provided about the size of the nucleus, the size of the alpha particle, and the interaction between nuclei and alpha particles. Concerning the radius of the nucleus and of the alpha particle: the Blair models fit the experimental data when the radius of the nucleus is about 1.5×10^{-13} $A^{\frac{1}{3}}$ cm and the radius of the alpha particle is 2×10^{-13} cm.[2,3,5] The Ford-Wheeler model fits the experimental data when the nuclear radius is $1.3\times10^{-13}A^{\frac{1}{3}}$ cm and the alpha-particle radius is about 2.5×10^{-13} cm. Either of these sets of values is in agreement with the currently accepted range of values.

The situation concerning the interaction between the alpha particle and the nucleus is not as clear. The exact form of the nuclear potential corresponding to the Blair model is not apparent but it does imply in some sense an opaque nucleus. On the other hand, the Ford-Wheeler model is based on the assumption that the rim of the nucleus is transparent. (No assumption need be made about the interior of the nucleus.) The predictions of the former model fit the data at small scattering angles. The predictions of the latter model fit the data at large scattering angles.

Information about the interaction of the alpha particle and the nucleus may also be derived from other experiments. For instance, the cross section for the production of neutrons from heavy elements bombarded by 40-Mev alpha particles is of the order of the geometrical area of the nucleus.[12] This implies that the nucleus is reasonably opaque to the alpha particle, but is not in disagreement with the existence of a transparent rim.

In order to obtain more exact information on the sizes of the nucleus and the alpha particle, and the interaction between the nucleus and the alpha particle, it will probably be necessary to compare the experiments with an exact calculation utilizing Coulomb wave functions and a complex nuclear potential with a diffuse edge.

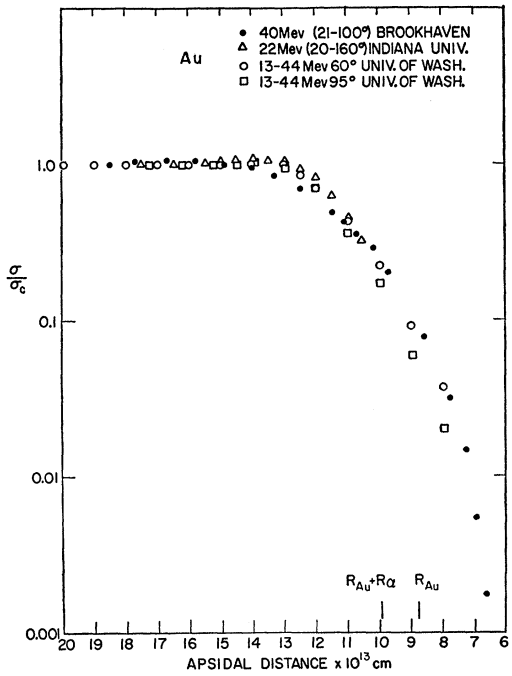

FIG. 11. σ/σ_c for Au as a function of apsidal distance.

6. ACKNOWLEDGMENTS

The authors would like to express their appreciation to the Brookhaven 60-inch cyclotron group. We would like to thank Professor K. W. Ford for generously supplying the results of computer calculations for the strong absorption models, for providing a summary of the unpublished Ford-Wheeler model, and for fitting the curves calculated from the latter model to the data of this experiment. We are indebted to Dr. C. E. Porter and Professor V. F. Weisskopf for many informative and stimulating discussions.

[12] Eisberg, Igo, and Wegner (to be published).